International Journal of Heat and Technology
Vol. 43, No. 2, April, 2025, pp. 625-632
Journal homepage: http://iieta.org/journals/ijht

Enhancing Gas Turbine Blade Cooling Efficiency: A Computational Fluid Dynamics Study of Turbulator Impact

Hameed Muqdad Rashid Hameed*, Mohd Faridh Ahmad Zaharuddin

Faculty of Mechanical Engineering, Universiti Teknologi Malaysia, Johor Bahru 81310, Malaysia

Corresponding Author Email: hameed@graduate.utm.my

https://doi.org/10.18280/ijht.430223

Received: 15 January 2025
Revised: 30 March 2025
Accepted: 14 April 2025
Available online: 30 April 2025

Keywords:
gas turbine, blade, cooling channel, Reynolds number, Nusselt number

ABSTRACT

By using ANSYS Fluent Turbine, this study replicates the cooling of turbine blades. Simulate the symmetrical structure of the turbine blade cooling channel to simplify the problem model. The primary objective of this study is to characterize thefluid flow and heat transfer properties within the cooling blade channel. As a result, the model's simulation and boundary conditions are defined in such a way that the fluidbehavior is concentrated on heat transfer. The cooling mechanism in this model is defined as cool airflow through an empty region in the blade's inner sides. The downstream wall is subjected to uniform heat flow, while the remainder of the wall istreated as an adiabatic surface. The flow had a Reynolds number (Re) range of 5,000 to 20,000. We solved the governing equations using the RNG k-turbulent model. Thefriction factor, Nusselt number, and skin friction are all affected by the turbulator height. The result indicates that the inclusion of a turbulator has a considerable effect on the cooling channel's performance. The presence of a turbulator within the coolingroute increases the rate of heat transfer, and the increase is proportional to the form and size of the turbulator. When a trapezoidal turbulator was introduced into a smoothchannel, the Nusselt number increased considerably.

1. INTRODUCTION

Gas turbines, alternatively referred to as combustion turbines, are a type of internal combustion engine. It converts chemical energy generated by the combustion of fuel to mechanical work using a continuous flow of gaseous working fluid [1-3]. Mechanical work can be used in any industrial application, while the ejected gaseous fluid can be used to provide thrust for propulsion. Due to its reliability and high power-to-weight ratio, the gas turbine has a wide range of applications. The only disadvantageof this method is that it is more expensive and less efficient than reciprocating engines.It is applicable to a variety of industries, including power generation, oil and gas, process plants, aviation, and marine applications. The demand for electricity from these uses is increasing at a constant rate [4, 5]. As a result, increasing turbine efficiency is a primary objective of all research endeavors in this area. As seen in Figure 1.

The gas turbine operates on the Brayton cycle principle. Cycles are classified as closed or open, depending on whether exhaust gas from the turbine output is recirculated, as seen in Figure 2. Fresh air at ambient pressure and temperature is pulled into the compressor, where its pressure and temperature are increased. This highly compressed air then passes into the combustion chamber, where the fuel is burned at a constant pressure, producing high-temperature pressurized gases. These gases flow through the turbine and expand to air pressure, generating useful work. Theideal Brayton cycle depicted in Figure 3 consists of four internally reversible phases. At point 1, ambient air is taken into the system and compressed entropically to a veryhigh pressure range from 15 to 35 atm. Fuel is burned in the combustion chamber withhigh-pressure air, with preferably no pressure loss between points 2 and 3. The fuel isinitially burned with less than one-third of the air present, and the combustion productsare subsequently mixed with the remaining air. The hot gases emerging from the turbine stator and rotor combustor expand entropically between points 3 and 4, resulting in the turbine rotating. A portion of the work is extracted for the purpose of compressing air, while the remainder is used for other purposes [6, 7]. In an open cycle, hotgases from the turbine are expelled without being recirculated back into the system. Incontrast, a closed-cycle gas turbine replaces the combustion process with constant pressure heat addition and the exhaust process with constant pressure heat rejection. The Brayton cycle is a closed-loop ideal cycle. The Brayton cycle P-v and T-s diagramsin Figure 3 summarize all four internally reversible processes [8-10].

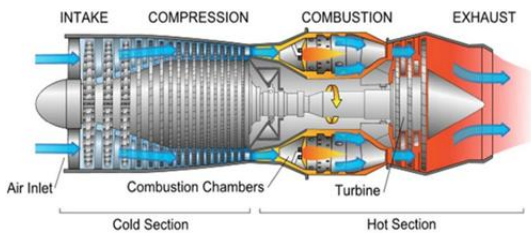

Figure 1. Gas turbine schematic

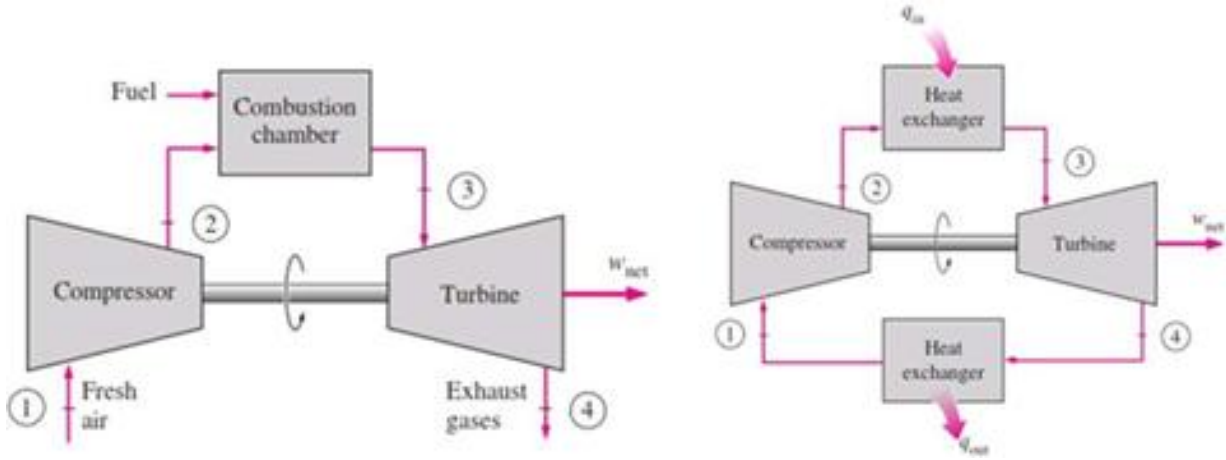

Figure 2. Gas turbine cycle. left: open cycle. right: closed-cycle turbine schematic

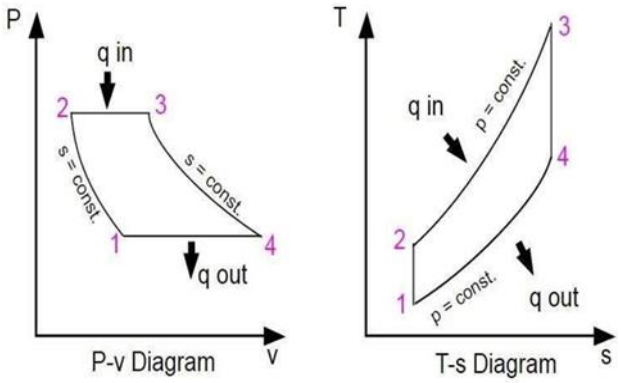

Figure 3. Brayton cycle

This paper organizes the remaining sections as follows: Section 2 discusses recent turbine cooling strategies. Section 3 describes numerical modeling methods, mesh independence, and validation. Section 4 explores how turbulator geometry and height affect flow and heat transfer characteristics. Section 5 wraps up the study by noting major findings and implications.

2. LITERATURE REVIEW

Continuous performance enhancement of gas turbine systems requires a continual increase in turbine intake temperatures. Turbine component cooling becomes a significant issue. One way to endure such a high temperature is to employa sophisticated material with a high melting point, however, this has limitations due tothe extremely high gas temperature. Numerous internal and external cooling technologies are employed to get the temperature of the turbine metal below its meltingpoint. Internal cooling is accomplished by circulating relatively cold air collected fromthe compressor bleed via the turbine blades' internal serpentine tunnels, as seen in Figure 4. Internal cooling is accomplished through both jet impingement and pin-fincooling [11-13]. External cooling, also known as film cooling, is a method of cooling that occurs outside of the body.

The following section outlines general (non-formatting) guidelines to follow. These guidelines are applicable to all authors and include information on the policies and practices relevant to the publication of your manuscript.

For several decades, substantial research on gas turbine blade cooling has beendone. Turbine blade cooling resulted in a significant reduction in blade temperature and an increase in blade lifetime of only a few percent. The cause for the minimal improvement was due to the cooling holes being placed incorrectly for a turbine blade that was not cooled andone that had internal cooling channels [14, 15]. They carried out their analysis using three distinct solvers:

1) a Navier–Stokes solver in the case of external flow and heat flux, 2) a finiteelement analysis (FEA) of the heat transfer and stress distribution within the solid, and 3) a one-dimensional aerothermal model for cooling ducts with roughened ribs [16, 17].

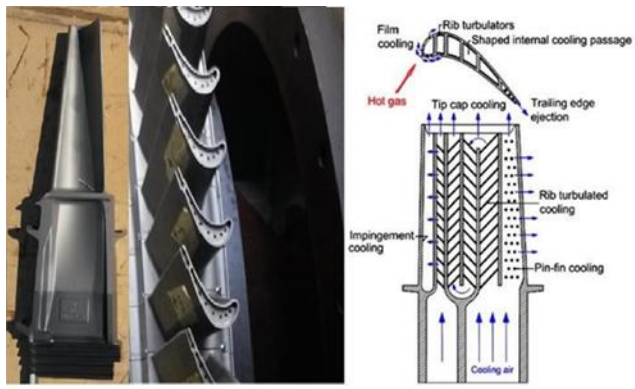

Figure 4. Internal cooling

3. METHODOLOGY

3.1 Structure of the ANSYS/FLUENT code

ANSYS/FLUENT is a commercial computational fluid dynamics (CFD) code that was developed in 1970. It is a general-purpose program for simulating structural and physical interactions, fluid dynamics, vibrations, chemical processes, and heat transport, among other phenomena. In a nutshell, ANSYS/FLUENT is a computer-aided engineering (CAE) application. This research utilizes the most recent version ofANSYS/FLUENT software, starting with Version 14.5, and progressing to Version 15.0 and 16.2 as the research proceeds. CFD codes are generally based on numerical techniques that extract information about fluid flow phenomena. These scripts are divided into four sections:

(1) identification of the problem, (2) pre-processing, (3) resolution, and (4) post-processing. The flow chart in Figure 5

depicts the overall procedure for the ANSYS/FLUENT code.

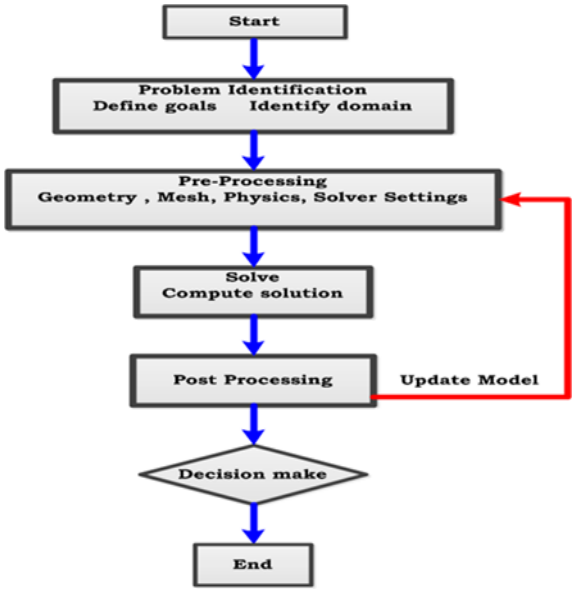

Figure 5. Flow chart showing the general procedure of the ANSYS/FLUENTcode (Fluent, A. N. S. Y. S., 2015)

3.2 Problem discretion

The governing equations for mass, momentum, and energy conservation were discretized using the finite volume technique (FVM), using a second-order upwind strategy for momentum and energy terms to improve accuracy. This work focuses on turbulator cooling, a type of impingement cooling, and tries to optimize the geometry of a gas turbine blade's cooling path. The stable RANS equations are solved using CFD analysis with Ansys/Fluent. The computationaldomain is represented by a long rectangular channel whose length is nine times its height. The turbulator is available in four different heights: 15 mm, 20 mm, 25 mm, and 30 mm. The diameter of the pitch is assumed to be 50 mm. The performance of several turbulator shapes, including triangular, trapezoidal, and circular, is investigated using numerical simulations with Reynolds numbers ranging from 5000 to 20,000. Theturbulator wall is subjected to a uniform heat flow of 800 W/m^2, air as the working fluid. The schematic diagram is present in Figure 6. The channel geometry is subjected to turbulent flow conditions using the *k-ε* turbulence model. Figure 6 depicts the schematic diagram.

The turbulent flow regime is simulated in this study using the RNG *k-ε* model, which is based on the Boussinesq hypothesis, which describes the relationship between the Reynolds tensor and the gradient of the mean velocity, the turbulent kinetic energy, and the turbulent viscosity [18, 19]. In the RNG *k-ε* model, to specify the turbulence specification method, the turbulence intensity and hydraulic diameter are used. I is defined as the Turbulence Intensity.

$$I = \frac{u^F}{u_{avg}} = 0.16\,(R_{eH})^{\frac{-1}{8}} \quad (1)$$

3.3 Grid independent study and code validation

The grids utilized in this investigation were produced using ANSYS V.20's meshing tool. The computing domain is divided into a uniform and non-uniform grid. A fine grid is used in the separation zone as well as at the channel's downstream wall due to the significant gradient in the flow's temperature and velocity components. Fourdifferent grids, as listed in Table 1, were evaluated to determine the effect of grid size on the computed results. The proportion of relative inaccuracy between the third and fourth grids was determined to be 2.445 percent, which can be ignored. As a result, the current study makes use of a grid of 214,000 points to save effort and processing time. The error percentage is calculated as follows:

$$e\% = \left|\frac{Q - Q_{n-1}}{Q_{n-1}}\right| \quad (2)$$

where, *Q* represents any quantity. A schematic diagram of the grid generatedin the transverse direction is present in Figure 7.

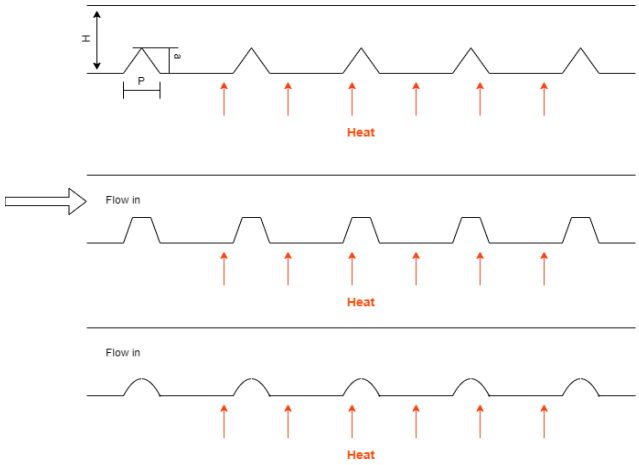

Figure 6. The schematic diagram of the cooling passage of the turbine blade

Table 1. Grid independent study

Grid No.	Grid Nodes	Nu	e%	u (ms^{-1})	e%	y$^+$
1	112,000	29.354	–	0.5621	–	0.645
2	138,000	30.928	2.446	0.5632	0.306	0.652
3	214,000	31.546	2.445	0.5655	0.334	0.732
4	378,000	31.921	0.085	0.5656	0.079	0.724

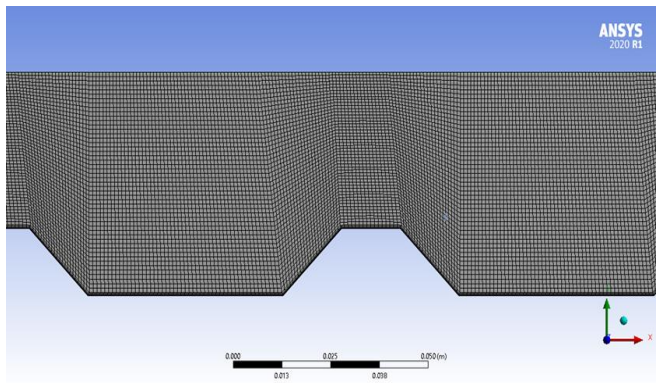

Figure 7. Mesh of the model

3.4 Validation

Due to facility constraints, experimental validation could

not be done at this time. However, our numerical model was rigorously verified against published data [20], yielding good agreement in Nusselt number and friction coefficient changes. Future work will include wind tunnel testing to support the existing findings, as shown in Figure 8.

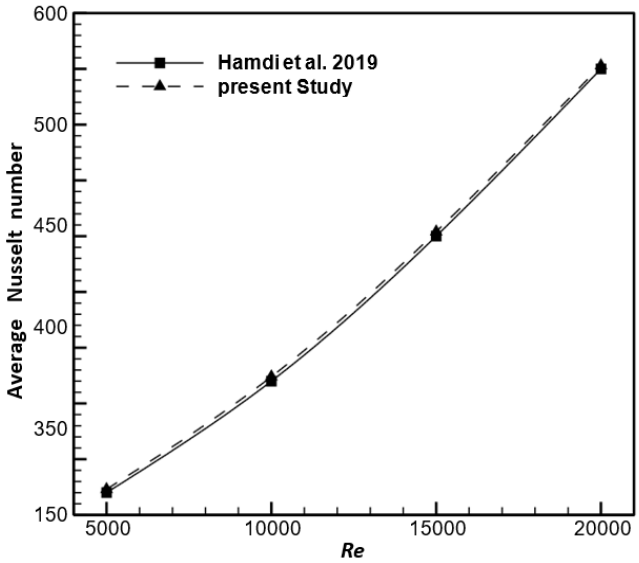

(a) Average Nusselt number

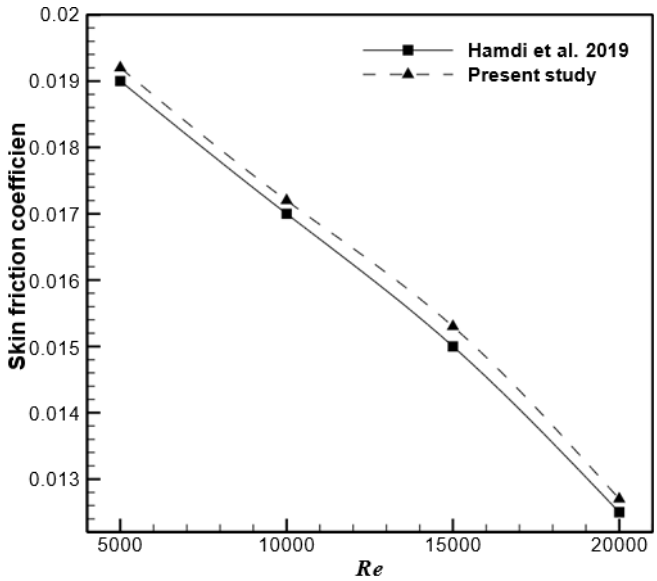

(b) Skin friction coefficient

Figure 8. Validation of the present CFD results for pure water with numerical data from previous studies: (a) average Nusselt number, (b) Skin friction coefficient

4. RESULTS AND DISCUSSION

The main objective of this numerical analysis is to investigate turbulent flow and heat transfer in a channel with a turbulator of triangular, circular, or trapezoidal shape with Reynolds numbers ranging from 5,000 to 20,000, turbulator heights of 15, 20, 25, and 30 mm, and a fixed pitch diameter of 50 mm. The first section of the analysis describes the numerical results of forced convective heat transfer and fluid flow over a channel with a variety of turbulators. This section discusses and evaluates the thermal and hydraulic efficiency implications of the turbulator form and Re.

4.1 The effect of turbulator shape on fluid flow and heat transfer

The addition of a turbulator to the channel had a significant effect on heat transfer and fluid flow, as illustrated in Figure 9(a) and Figure 9(b), which shows the surface Nusselt number and average skin friction coefficient along the channel's down wall for each channel at Re values ranging from 5,000 to 20000 and an amplitude height of 20 mm. The triangular turbulator had the highest Nusselt number compared to the other shapes, but the circular turbulator had the lowest Nusselt number. The circular turbulator has the lowest skin friction coefficient, followed by the triangular and trapezoidal turbulators.

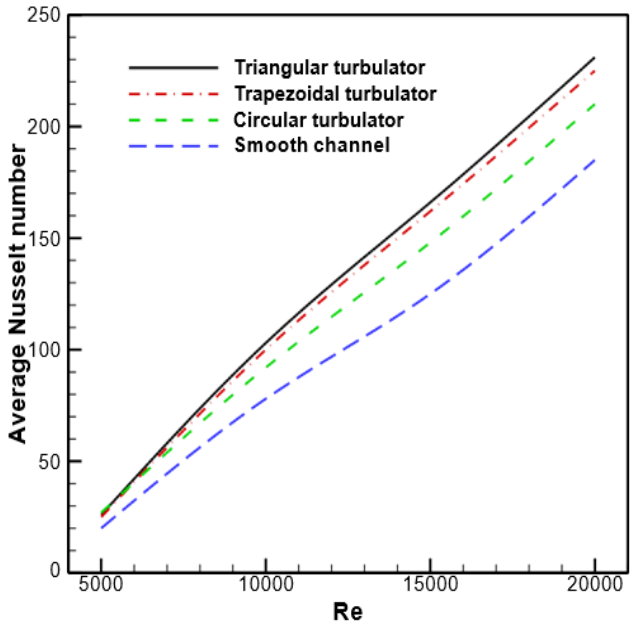

(a) Average Nusselt number

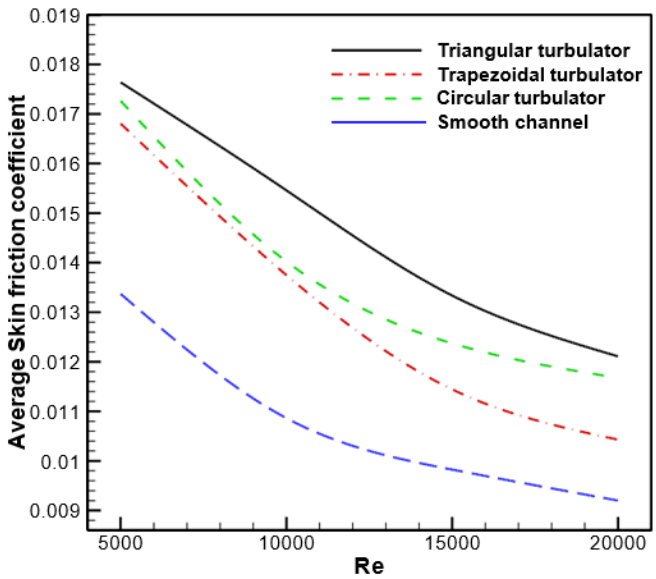

(b) Average skin friction for different turbulator shapes

Figure 9. (a) Average Nusselt number, (b) average skin friction for different turbulator shapes

The Nusselt number grows as the Reynolds number increases, as illustrated in Figure 9(a). This is owing to the turbulator's vortex, which contributes to an increase in the heat

transfer ratio. Increased flow rate results in a thinner boundary layer and lower thermal resistance, which results in an increased heat transfer rate. At extremely high Reynolds numbers, this boost becomes significant.

According to Figure 9(b), the average skin friction coefficient of all turbulators is the same. The enhancement of heat transmission was related to flow difficulties, and flow after the turbulator generated a larger recirculation area and a thin boundary layer.

Figure 10 illustrates the effect of various turbulator shapes on the velocity distribution at Re = 5,000, pitch diameter = 50 mm, and turbulator height = 20 mm.

The velocity streamline was significantly influenced by the converging and diverging sections of the turbulator walls. Due to the sharp edge of the curved wall, a stable vortex was generated at the diverging region of the turbulator wall of each shape.

The trapezoidal turbulator channel has the greatest velocity gradient behind the turbulator. This increase in velocity gradient results in a narrower thermal boundary layer at the trapezoidal turbulator wall's converging portion. Due to the tension between the wall and viscous sublayers, the velocity of the walls remains low. However, the addition of turbulator walls to the cooling blade channel improves the velocity distribution near the wall, resulting in a more uniform mixing of the flow layers.

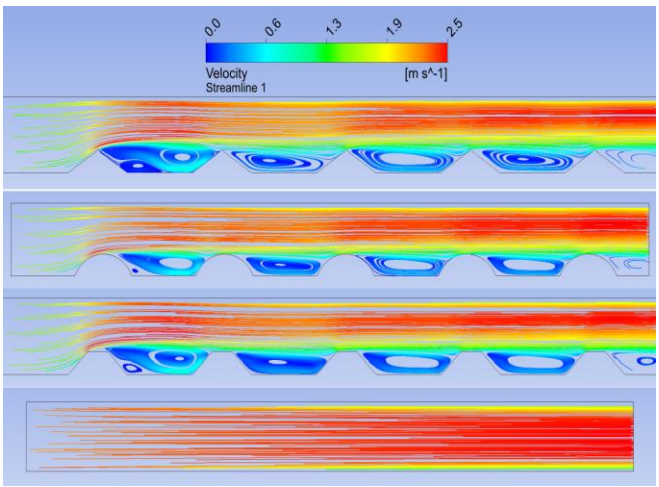

Figure 10. Velocity steam line contour for different turbulator shape

Figure 11 illustrates the influence of several turbulator designs, including trapezoidal, triangular, and circular walls, on the isothermal contour at Reynolds number = 5000, a turbulator height of 20 mm, and a pitch diameter of 50 mm. The isothermal contour of the turbulator walls reveals that the thickness of the thermal boundary layer varies with the turbulator shape, resulting in a variation in flow mixing and surface area. As a result, depending on the turbulator design, the temperature gradient at the wall will rise or decrease, eventually affecting the heat transfer enhancement. The same graphic demonstrates that the trapezoidal turbulator wall has a greater temperature gradient than the triangular corrugated and circular turbulator walls. The isothermal contour's principal pattern indicates a reduction in the thermal boundary layer following the first turbulator, where this point represents the initial recirculation zone formed by the turbulator. However, due to flow mixing and the secondary vortex formed by the turbulator walls, the boundary layer thickness begins to expand again.

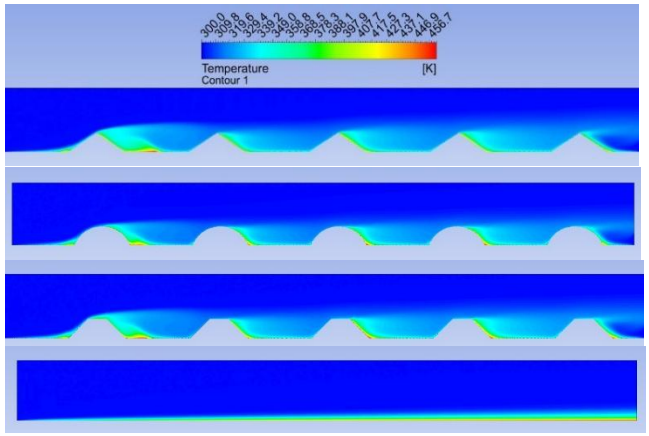

Figure 11. Temperature distribution contour for different turbulator shapes

Figure 10 shows that the triangular turbulator creates stronger flow separation and recirculation zones near the wall, encouraging turbulent mixing and hence increasing local heat transfer. Figure 11 demonstrates that trapezoidal turbulators produce sharper temperature gradients, indicating thinner thermal boundary layers that cause higher convective heat flux.

The influence of Reynolds number on PEC is seen in Figure 12 for triangular, trapezoidal, and circular turbulator designs. The trapezoidal shape has a higher PEC value than the other shapes due to a significant increase in heat flow across that channel. In comparison, the PEC increased with an improvement of Re. PEC reached is seen in Figure 12 for triangular, trapezoidal, and circular turbulator designs. The trapezoidal shape has a higher PEC value than the other shapes due to a significant increase in heat flow across that channel. In comparison, the PEC increased with an improvement of Re. PEC reached a high of 1.25 at Re = 20,000 and a trapezoidal turbulator shape, while it reached a minimum of 1.05 at Re = 10,000 and a circular turbulator shape. By adding a turbulator wall to the cooling blade channel, PEC is significantly improved.

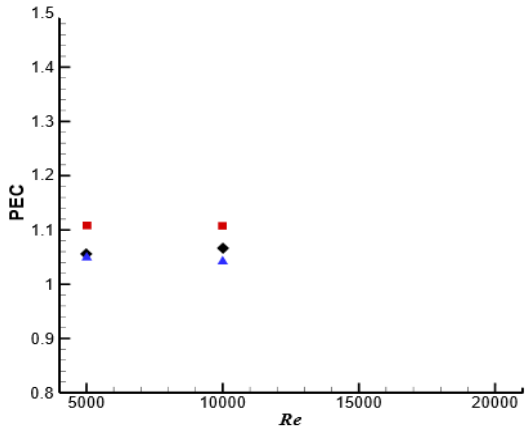

Figure 12. PEC for different turbulator shapes

In general, PEC increases with flow rate because the friction factor falls with Reynolds number due to the fact that the thickness of the boundary layer is significantly affected by flow rate at low Reynolds numbers.

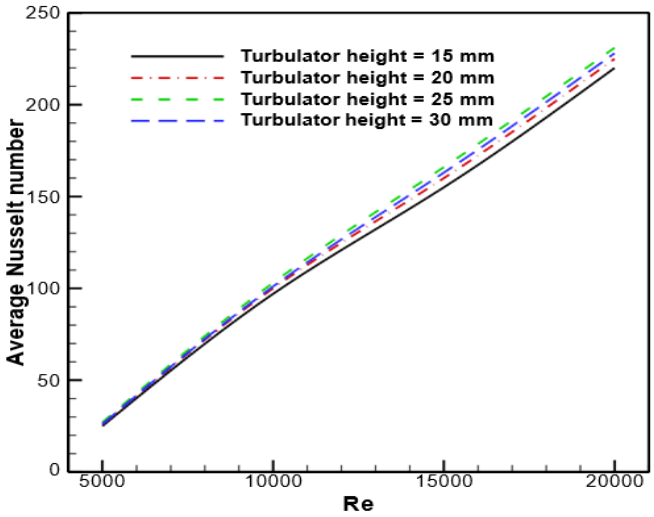

(a) Average Nusselt number

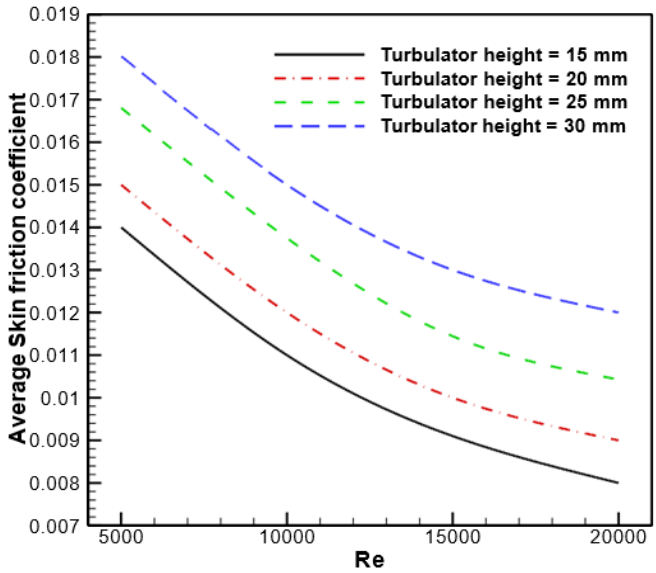

(b) Average skin friction for different turbulator heights

Figure 13. (a) Average Nusselt number, (b) average skin friction for different turbulator heights

4.2 The effect of turbulator height on fluid flow and heat transfer

The numerical results of the average skin friction and Nusselt number at different turbulator heights and Reynolds numbers are presented in this section. The influence of different amplitude heights (15, 20, 25, and 30 mm) on the average Nusselt number for a trapezoidal turbulator wall with a pitch diameter of 50 mm and a Reynolds number in the range of 5000 to 20000 is shown in Figure 13(a). The simulation findings indicate that when the turbulator height of the trapezoidal turbulator increases, the average Nusselt number increases along with the friction factor. This increase in Nu is attributable to the downstream section's promotion of the improved temperature and fluid mixing gradients as the turbulator height increases. It is worthy to be mentioned here that the two highest heights of the turbulator height show approximately the same heat transfer rate while they provide a higher enhancement in the heat transfer compared to the smooth channel. However, as illustrated in Figure 13(b), the increase in the average Nu reaches a maximum at turbulator height = 25 mm, whereas the friction factor continues to climb as the amplitude height increases (b). It is worth noting here that the two highest turbulator heights exhibit nearly the same heat transfer rate while providing a greater heat transfer increase than the smooth channel.

Furthermore, the intensity of the vortex increases with the increase of the turbulator height. Figure 14 illustrates the effect of turbulator characteristics, namely turbulator height, on the distribution of flow velocity at Re 5,000. The result suggested that the turbulator wall has a considerable effect on the velocity streamline gradient at the center of each diverging segment. The streamlines of velocity grew and reduced in size when the turbulator setting was changed. The finding indicates that as the turbulator height grows in the core of each divergent section, the recirculation zone is impacted. Additionally, the intensity of the vortex increases as the turbulator height increases.

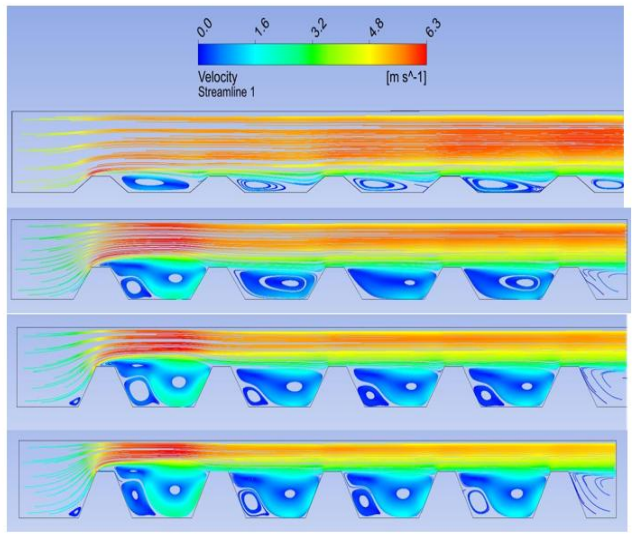

Figure 14. Velocity steam line contour for different turbulator heights

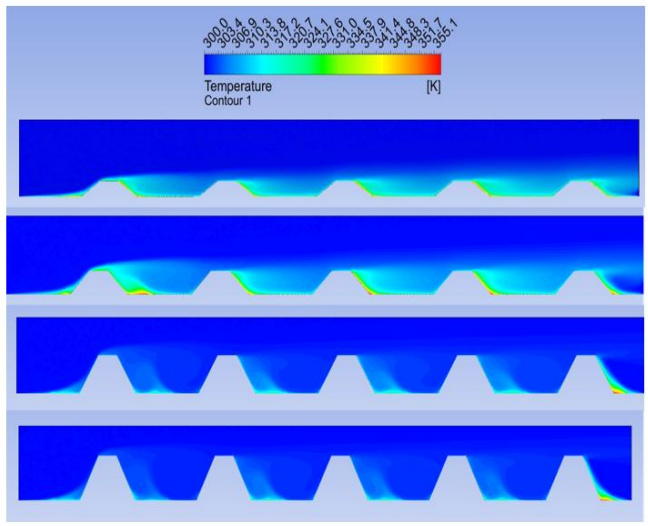

Figure 15. Temperature distribution contour for different turbulator heights

At Reynolds number Re equal 5,000, Figure 15 illustrates the influence of various turbulator heights (15, 20, 25, and 30 mm) and a 50 mm wavelength on the isothermal contour of the cooling blade channel combined with the trapezoidal turbulator wall. It was discovered that increasing the turbulator

height had a substantial effect on the temperature gradient distribution because the secondary vortex strength increases and encourages fluid mixing in the core of each divergence section. Additionally, the result indicates that there is no discernible change in the thermal boundary layer after turbulator height = 25 mm, as the channel's maximum fluid mixing occurs at turbulator height = 25 mm. Additionally, the thickness of the thermal boundary layer grows with increasing turbulator height at the diverging section for the same reason. Increased temperature gradients should result in an increase in heat transfer rate.

Table 2 presents a comparative analysis of the three turbulator geometries, revealing that while the triangular shape offers the highest Nusselt number, the trapezoidal shape provides the best PEC due to balanced heat transfer and pressure loss.

Table 2. Comparison

	Triangular	**Trapezoidal**	**Circular**	**Smooth**
Nusselt number	240	230	210	180
Skin friction	0.0179	0.0169	0.0172	0.0135
PEC	1.08	1.25	1.05	0

5. CONCLUSIONS

The present study numerically evaluated fluid flow and the heat transfer performance behavior in a rectangular passage of a gas turbine blade using air as the working fluid. Three distinct turbulator shapes were evaluated within a rectangular channel, as well as the effect of turbulator shape on heat transmission and fluid flow parameters. The numerical study was conducted using the *k-ω* turbulence model. Additionally, the influence of the turbulator height was examined. It was discovered that the inclusion of a turbulator had a considerable effect on the cooling channel's performance. The presence of a turbulator within a cooling route increases the rate ofheat transfer, and the increase is proportional to the form and size of the turbulator. When a trapezoidal turbulator was introduced into a smooth channel, the Nusselt number increased considerably.

The results indicated that adding a turbulator wall to the channel significantly increased heat transfer. Additionally, it has been demonstrated that the trapezoidal turbulator wall has the highest value of PEC = 1.25, which is a factor of the Nusselt number and friction factor.

The turbulator height has a direct effect on the rate of heat transfer, with a greater turbulator height resulting in a faster rate of heat transfer. The trapezoidal turbulator with a pitch of 50 mm and a diameter of 25 mm a maximizes heat transfer. As a result of the improved mixing of the flow, the subrecirculation zones generated by the turbulator wall of the trapezoidal boost heat transmission. As the Nusselt number (Nu) increases and the Reynolds number (Re) increases, as well, resulting in a dramatic fall in the friction factor.

Among all investigated geometries, the trapezoidal turbulator at 25 mm height had the best thermal-hydraulic performance, with a PEC of 1.25. Triangular forms improved heat transfer the greatest, but their greater friction factor reduced efficiency. In contrast, circular shapes exhibited the lowest pressure drop but fared poorly in heat transfer. The trapezoidal shape provides a balanced design for practical use in turbine blade cooling systems.

REFERENCES

[1] Soltanloo, M., Hossein Babaei, M., Porhonar, M., Shajari, Y., Seyedraoufi, Z.S., Jahangiri, M.R. (2025). Root cause failure analysis of 320 MW steam turbine: Visual, metallurgical, and mechanical approach. http://doi.org/10.2139/ssrn.5139321

[2] Guzović, Z., Kastrapeli, S., Budanko, M., Klun, M., Rašković, P. (2024). Improving the thermodynamic efficiency and turboexpander design in bottoming organic Rankine cycles: The impact of working fluid selection. Energy, 307: 132642. http://doi.org/10.1016/j.energy.2024.132642

[3] Kislat, O., Römgens, J., Schuldt, S., Zanger, J., Jakobs, N., Henke, M., Kraus, C., Moosbrugger, A., Asmi, M.A., Aigner, M. (2024). Development and testing of a gas turbine test rig setup for demonstrating new aviation propulsion concepts. Aerospace, 11(7): 534. http://doi.org/10.3390/aerospace11070534

[4] Spodniak, M., Semrád, K., Draganová, K. (2021). Turbine blade temperature field prediction using the numerical methods. Applied Sciences, 11(6): 2870. http://doi.org/10.3390/app11062870

[5] Shi, D.B., Liao, G.Q., Meng, Y., Zhang, D., Xie, Y.H. (2024). Degradation performance rapid prediction and multi-objective operation optimization of gas turbine blades. Energy, 305: 132195. http://doi.org/10.1016/j.energy.2024.132195

[6] Cockcroft, C.C., Le Roux, W.G. (2025). The influence of applying turbine inlet air cooling to a small-scale parallel-flow Brayton cycle. Energy Conversion and Management, 325: 119407. http://doi.org/10.1016/j.enconman.2024.119407

[7] Van der Merwe, A.H., Le Roux, W.G., Humphries, E.D. (2023). Parallel turbochargers for small-scale power generation. Applied Thermal Engineering, 235: 121410. http://doi.org/10.1016/j.applthermaleng.2023.121410

[8] Cockcroft, C.C., Le Roux, W.G. (2025). A comparative analysis between small-scale recuperated parallel-flow Brayton cycles. Applied Thermal Engineering, 267: 125837. http://doi.org/10.1016/j.applthermaleng.2025.125837

[9] Sodhro, A.A., Lemma, T.A., Gilani, S.I.U.H., Salilew, W.M. (2024). Comparative performance analysis of gas turbine with and without intercooler using natural gas and hydrogen fuels. Engineering, Technology and Applied Science Research, 14(6): 18283-18289. http://doi.org/10.48084/etasr.8825

[10] Madu, K.E., Nwanze, N.E., Igbagbon, E.J., Emu, A.O. (2025). Integration of a high-pressure fogging air intake cooling system in a gas turbine power plant. Journal of Applied Sciences and Environmental Management, 29(4): 1295-1302.

[11] M., W.A., Yousif Khenyab, A., Shaker, L.M., Kdhim, R.H. (2023). Overview of a gas turbine blades power plant. Al-Salam Journal for Engineering and Technology, 3(1): 117-127. http://doi.org/10.55145/ajest.2024.03.01.010

[12] Chang, S.W., Lu, Y.E., Wan, T.Y. (2024). Cooling improvement by internal effusion jets for impingement

pin-fin channel. International Journal of Thermal Sciences, 206: 109315. http://doi.org/10.1016/j.ijthermalsci.2024.109315
[13] Hu, L.B., Rao, Y., Zhang, H. (2024). Numerical study of film cooling at the outlet of gas turbine exhaust. Journal of Physics: Conference Series, 2838(1): 012024. http://doi.org/10.1088/1742-6596/2838/1/012024
[14] Zha, H., Xu, Y.Q., Tang, Z.G., Li, B., Wang, D.Z. (2024). Conjugate heat transfer advancements and applications in aerospace engine technology. Applied Sciences (Switzerland), 14(9): 3556. http://doi.org/10.3390/app14093556
[15] Liu, J., Wang, J.B., Yang, K. (2024). Heat transfer enhancement in a triple-layered turbine blade internal cooling channel. Applied Thermal Engineering, 248: 123341. http://doi.org/10.1016/j.applthermaleng.2024.123341
[16] Wang, S.Y., Li, X.Y., Ren, J. (2023). Comprehensive evaluation on conjugate heat transfer and thermal stress performance of film cooling. http://doi.org/10.2139/ssrn.4524906
[17] Yildiz, E., Koca, F., Can, I. (2025). Optimal design and analysis of the cooled turbine blade in gas turbines with CFD. Journal of Applied Fluid Mechanics, 18(1): 60-72. http://doi.org/10.47176/jafm.18.1.2853
[18] Shahbazi, A.A., Esfahanian, V. (2025). Improving turbulence modeling for gas turbine blades: A novel approach to address flow transition and stagnation point anomalies. Journal of Computational Physics, 520: 113499. http://doi.org/10.1016/j.jcp.2024.113499
[19] Kumar, A., Bharti, R.P. (2024). Assessment of RANS-based turbulence models for isothermal confined swirling flow in a realistic can-type gas turbine combustor application. Journal of Computational Science, 81: 102362. http://doi.org/10.1016/j.jocs.2024.102362
[20] Ahmed, H.E., Salman, B.H., Kerbeet, A.S. (2019). Heat transfer enhancement of turbulent forced nanofluid flow in a duct using triangular rib. International Journal of Heat and Mass Transfer, 134: 30-40. http://doi.org/10.1016/j.ijheatmasstransfer.2018.12.163

NOMENCLATURE

CFD	computational fluid dynamic
C_f	skin friction coefficient
e%	error percentage
PEC	performance evaluation criteria
Q	quantity
RANS	Reynolds average Navier stokes
Re	Reynolds number
TBC	turbine blade coating
V^+	fluid velocity